

# Preparation of Zeolite-Incorporated Poly(dimethyl siloxane) Membranes for the Pervaporation Separation of Isopropyl Alcohol/Water Mixtures

Arjumand A. Kittur, Mahadevappa Y. Kariduraganavar, Srikant S. Kulkarni, Mrityunjaya I. Aralaguppi

Department of Chemistry and Center of Excellence in Polymer Science, Karnatak University, Dharwad 580003, India

Received 11 October 2004; accepted 17 November 2004

DOI 10.1002/app.21566

Published online in Wiley InterScience (www.interscience.wiley.com).

**ABSTRACT:** ZSM-5 zeolite-incorporated poly(dimethyl siloxane) membranes were prepared, and the molecular dispersion of the zeolite in the membrane matrix was confirmed with scanning electron microscopy. After the swelling of the membranes was studied at 30°C, the membranes were subjected to the pervaporation separation of isopropyl alcohol/water mixtures at 30, 40, and 50°C. The effects of the zeolite loading and feed composition on the pervaporation performances of the membranes were analyzed. Both the permeation flux and selectivity increased simultaneously with increasing zeolite content in the membrane matrix. This was examined on the basis of the enhancement of hydrophobicity, selective adsorption, and the establishment of molecular sieving action. The membrane containing the highest zeolite loading (30 mass %) had the highest separation selectivity (80.84) and flux ( $6.78 \times 10^{-2} \text{ kg m}^{-2} \text{ h}^{-1}$ ) at 30°C with 5 mass % isopropyl alcohol in the feed. From the temperature dependence of the diffusion and permeation values, the Arrhenius activation parameters were estimated. A pure membrane exhibited higher activation energy values for permeability ( $E_p$ ) and diffusivity ( $E_D$ ) than zeolite-incor-

porated membranes, and signified that permeation and diffusion required more energy for transport through the pure membrane because of its dense nature. Obviously, the zeolite-incorporated membranes required less energy because of their molecular sieving action, which was attributed to the presence of straight and sinusoidal channels in the framework of the zeolite. For the zeolite-incorporated membranes, the activation energy values obtained for isopropyl alcohol permeation were significantly lower than the water permeation values, and this suggested that the zeolite-incorporated membranes had higher selectivity toward isopropyl alcohol. The  $E_p$  and  $E_D$  values ranged between 21.81 and 31.12 kJ/mol and between 15.27 and 41.49 kJ/mol, respectively. All the zeolite-incorporated membranes exhibited positive values of the heat of sorption, and this suggested that the heat of sorption was dominated by Henry's mode of sorption. © 2005 Wiley Periodicals, Inc. *J Appl Polym Sci* 96: 1377–1387, 2005

**Key words:** activation energy; membranes; selectivity; zeolites

## INTRODUCTION

During recent decades, several studies have indicated that pervaporation (PV) is a promising technique for the removal of organic liquids from water.<sup>1</sup> This feature is very important in many applications, such as the treatment of organic-contaminated wastewater, the harvesting of organic substances from fermentation broths, and the recovery of valuable organic compounds from side-stream processes,<sup>2</sup> including the separation of azeotropic mixtures,<sup>3,4</sup> the separation of organic–organic liquids,<sup>5,6</sup> the dehydration of organic solvents,<sup>7,8</sup> and the continuous removal of one of the products of a reaction from a

bioreactor.<sup>9</sup> In PV, the separation of two or more components is accomplished across a membrane by the combination of two phenomena: the difference in the diffusion rates through the thin polymer membrane and an evaporative phase change similar to a simple flash-distillation step. Thus, PV is considered to be a less energy-intensive operation than distillation, with which it often competes industrially.

Isopropyl alcohol (IPA) is widely used in the electronic and liquid-crystal-display industries for cleaning and drying operations during the production of semiconductors, flat-panel displays, disks, optoelectronics, and other electronic components.<sup>10,11</sup> Because of escalating virgin-chemical costs, disposal costs, and safety and environmental concerns, the reprocessing of IPA has become an attractive, practical, and cost-effective source for recycling ultrapure IPA. Obtaining IPA in its pure form is difficult because it forms an azeotrope at a 14.7 mass % water concentration.<sup>12</sup> Hence, its separation by conventional distillation methods, such as solvent extraction and rotavaporation, or by distilla-

Correspondence to: M. Y. Kariduraganavar (mahadevappak@yahoo.com).

Contract grant sponsor: Department of Science and Technology (New Delhi, India); contract grant number: SP/S1/H-31/2000.

tion could prove uneconomical. Recently, several membrane materials have been modified for the separation of IPA from its aqueous mixtures through PV.<sup>10–13</sup> However, the membranes employed in such separation studies often yield compromised values of the flux and selectivity because of a tradeoff phenomenon existing between the flux and separation factor in PV.

Elastomers have a glass-transition temperature below the ambient temperature. The polymer chains of elastomers contain rather small side groups, which are nonpolar. This results in a flexible structure, which preferentially permeates organic liquids. Therefore, membranes made up of elastomeric material are best suited for the selective removal of organics from water. One of the most common elastomers is poly(dimethyl siloxane) (PDMS), and it is widely accepted as a membrane material for the PV separation of organics from their aqueous streams.<sup>2</sup> On the other hand, zeolites have a high surface area (up to 1000 m<sup>2</sup>/g), a high void volume (30% of the total volume of the zeolite), and a uniform pore size distribution, and so these have been used widely as shape-selective catalysis and separation media in chemical and physical processes.<sup>14</sup> Thus, the incorporation of selective zeolites into a suitable polymeric membrane matrix can improve the separation performance of PV membranes because of a combined influence of molecular sieving action, selective adsorption, and differences in the diffusion rates.<sup>14–16</sup> Furthermore, zeolites have high mechanical strength and good thermal and chemical stability, and so the membranes prepared with these zeolites can be used over a wide range of operating conditions. To explore the possibility of zeolites in membrane materials for continuous separation processes, many investigators have carried out pioneering investigations.<sup>17–21</sup> Hennepe et al.<sup>15</sup> showed that the selectivity of an organophilic membrane for a lower alcohol series could be improved substantially by the incorporation of silicalite zeolite into a PDMS membrane. Vankelecom et al.<sup>22</sup> also found that zeolite-filled PDMS membranes had a strong influence on the PV separation of alcohol/water mixtures.

This article reports the effect of ZSM-5 zeolite on PDMS membranes for the PV separation of water/IPA mixtures. The sorption and diffusion data are also discussed to provide qualitative insight into the transport phenomenon. From the temperature dependence of the permeation flux and diffusion coefficients, the Arrhenius activation parameters have been estimated. The results are discussed in terms of the PV separation efficiency of the membranes.

## EXPERIMENTAL

### Materials

Elastosil LR 7665A and Elastosil LR 7665B were kindly supplied by Wacker-Chemie GmbH (Hanns-Seidel-

**TABLE I**  
Physicochemical Properties of Hydrophobic  
ZSM-5 Zeolite<sup>22,23</sup>

Counterion	NH <sub>4</sub> <sup>+</sup>
SiO <sub>2</sub> /Al <sub>2</sub> O <sub>3</sub>	33
Density	1.76 g/mL
Pore size	0.54 nm
Pore volume	0.19 mL/g
Brunauer-Emmett-Teller	430 m <sup>2</sup> /g
Topology	MFI

Platz, München, Germany). IPA, methyl isobutyl ketone (MIBK), and ZSM-5 zeolite were purchased from S.D. Fine Chemicals, Ltd. (Mumbai, India). The characteristic properties of ZSM-5 zeolite are given in Table I. All the chemicals were reagent-grade and were used without further purification. Double-distilled water was used throughout the research.

### Membrane preparation

For the preparation of the virgin PDMS membrane, Elastosil LR 7665A was thoroughly mixed with Elastosil LR 7665B for 1 h at the ambient temperature in a 1:1 ratio. The mixed suspension was subjected to a vacuum treatment for 2 h to remove air bubbles. The resulting suspension was mechanically cast onto a clean glass plate and was allowed to cure at 150°C for 1 h to ensure complete crosslinking. The membrane was subsequently peeled off and was designated as M.

For the preparation of zeolite-incorporated PDMS membranes, a known amount of ZSM-5 zeolite was placed in 25 mL of MIBK, and this was dispersed by placement in an ultrasonic bath for 1 h at a fixed frequency of 38 kHz (Grant XB6, Cambridge, UK). After proper dispersion was ensured, the crosslinker (Elastosil LR 7665B) was added slowly while the MIBK solution was stirred, and this was followed by the addition of the prepolymer (Elastosil LR 7665A). After the addition, the stirring was continued for 2 h to achieve proper mixing. The rest of the procedure was similar to that for virgin membrane M. The amounts of the crosslinker and prepolymer were kept constant for each membrane. However, the concentration of ZSM-5 zeolite with respect to PDMS was varied at 10, 20, and 30 mass %, and the membranes thus obtained were designated as M-1, M-2, and M-3, respectively. The thickness of these membranes was measured at different points with a Peacock model G dial thickness gauge (Ozaki Mfg. Co., Ltd., Ozaki, Japan) with an accuracy of  $\pm 2 \mu\text{m}$ , and the average thickness was considered for calculation. The thickness of the membranes was  $80 \pm 2 \mu\text{m}$ .

### Membrane characterization

Scanning electron microscopy (SEM) observations of the membrane surfaces and cross sections were car-

ried out at 20 kV with a JSM-840A scanning microscope (JEOL, Tokyo, Japan). All specimens were coated with a conductive layer (400 Å) of sputtered gold.

### Swelling measurements

The equilibrium sorption experiments were performed in water/IPA mixtures of different compositions with an electronically controlled oven (WTB Binder, Tuttlingen, Germany). The masses of the dry membranes were first determined, and these were equilibrated by immersion in feed mixtures of different compositions in a sealed vessel at 30°C for 24 h. The swollen membranes were weighed as quickly as possible after careful blotting on a digital microbalance (Mettler B204-S, Toledo, Zurich, Switzerland) within a sensitivity of  $\pm 0.01$  mg. The degree of swelling (DS) was calculated as follows:

$$DS(\%) = \left( \frac{W_s - W_d}{W_d} \right) \times 100 \quad (1)$$

where  $W_s$  and  $W_d$  are the masses of the swollen and dry membranes, respectively.

### PV experiments

PV experiments were performed with an indigenously designed apparatus reported in our previous articles.<sup>12,24</sup> The effective surface area of each membrane in contact with the feed stream was 34.23 cm<sup>2</sup>, and the capacity of the feed compartment was about 250 cm<sup>3</sup>. The vacuum in the downstream side of the apparatus was maintained (10 Torr) with a two-stage vacuum pump (Toshniwal, Chennai, India). The IPA composition in the feed mixture was varied from 5 to 25 mass %. The test membrane was allowed to equilibrate for about 1 h while in contact with the feed mixture before the PV experiment was performed. After a steady state was attained, the permeate was collected in a trap immersed in a liquid-nitrogen jar on the downstream side at a fixed times. The experiments were carried out at 30, 40, and 50°C. The flux was calculated from the weight of the permeate, and its composition was estimated by the measurement of the refractive index with an accuracy of  $\pm 0.0001$  units with Abbe's refractometer (Atago-3T, Tokyo, Japan) and by comparison with a standard graph, which was established with known compositions of water/IPA mixtures. All the experiments were performed at least three times, and the results were averaged. The results of permeation for the water/IPA mixtures during PV were reproducible within the admissible range.

The membrane performance in the PV experiments was assessed in terms of the total flux ( $J$ ), separation factor ( $\alpha_{\text{sep}}$ ), and pervaporation separation index (PSI):

$$J = \frac{W}{At} \quad (2)$$

$$\alpha_{\text{sep}} = \frac{P_{\text{IPA}}/P_w}{F_{\text{IPA}}/F_w} \quad (3)$$

$$PSI = J(\alpha_{\text{sep}} - 1) \quad (4)$$

where  $W$  is the mass of the permeate (kg);  $A$  is the effective membrane area (m<sup>2</sup>);  $t$  is the permeation time (h);  $P$  and  $F$  are the mass percentages of the permeate and feed, respectively; and subscripts  $w$  and IPA denote water and isopropyl alcohol, respectively.

## RESULTS AND DISCUSSION

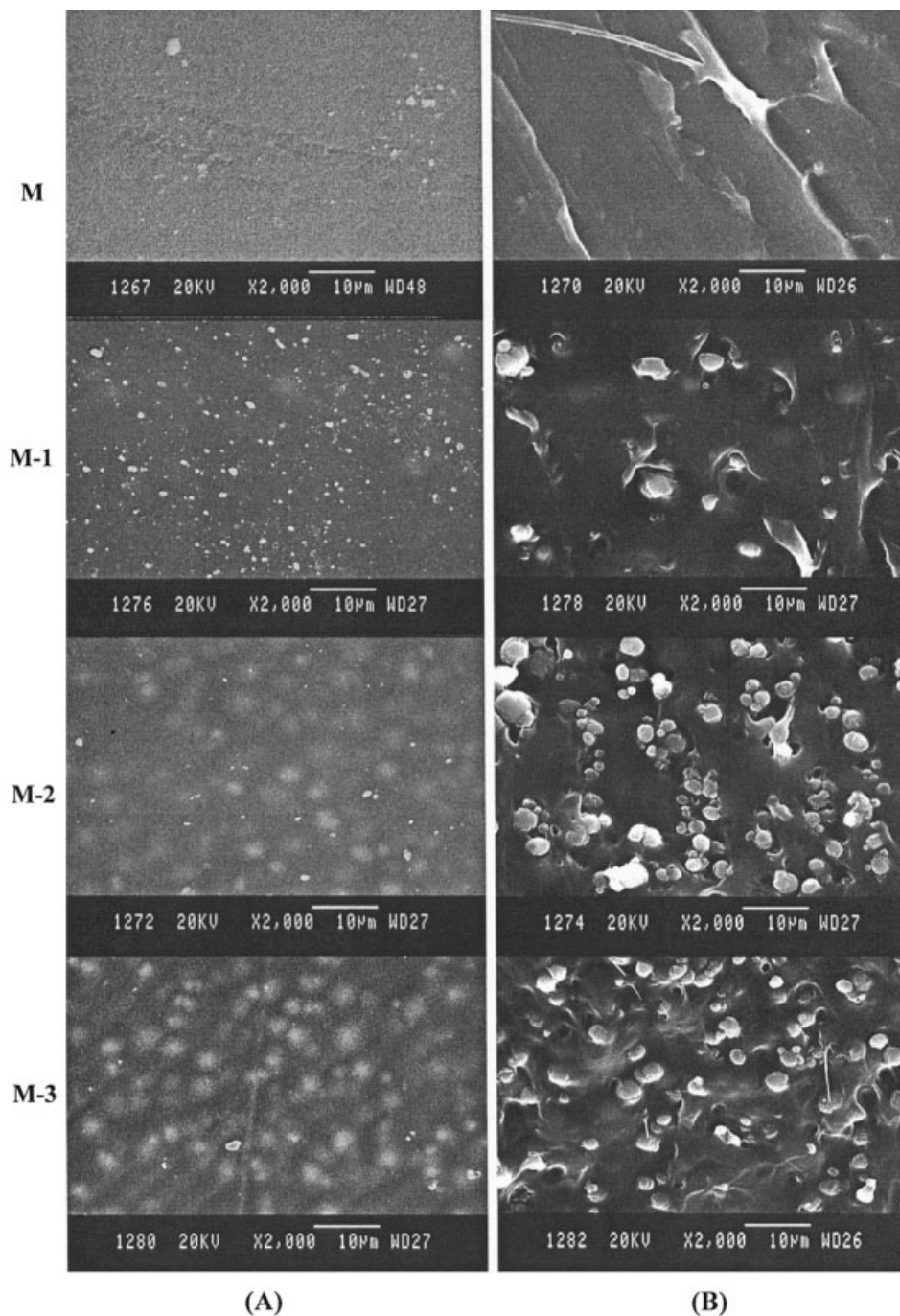
### SEM

Figure 1(A,B) presents SEM photographs of surface and cross-sectional views of the pure and zeolite-incorporated PDMS membranes. The micrographs confirm that the zeolite distribution increased from membrane M-1 to M-3 with increasing zeolite loading. The zeolite was distributed evenly throughout the membrane matrix, with no apparent clustering. Furthermore, the photographs clearly show that the zeolite crystals were embedded in the membrane matrix, with no voids around them. This ensured that the zeolite-incorporated membranes obtained here were free from possible defects.

### Effects of the feed composition and zeolite loading on the membrane swelling

The membrane swelling in certain liquids depends on the chemical composition and microstructure of the polymer and on the way in which the membrane interacts with the permeants.<sup>25</sup> Therefore, in the PV process, the degree of membrane swelling is an important factor that controls the transport of permeating molecules under the chemical potential gradient.

To study the effects of the feed composition and zeolite loading on the membrane swelling, we plotted the DS percentage for all the membranes with respect to different mass percentages of IPA in the feed, as shown in Figure 2. From a close inspection of the plot, we observed that DS increased markedly for all the membranes when the concentration of IPA was increased from 5 to 10 mass % in the feed. However, further increasing IPA in the feed did not increase the membrane swelling much, but it did increase marginally. This was because, at a lower concentration of IPA in the feed, the interaction between the molecules of water and IPA was less than that of IPA and the membrane matrix. However, when the concentration of IPA increased beyond 10 mass % in the feed, the interaction increased between the water and IPA molecules because of hydrogen-bonding interactions. This



**Figure 1** SEM photographs of pure and zeolite-incorporated membranes: (A) surface views and (B) cross-sectional views.

resulted in the formation of clusters, which might have relatively suppressed the diffusion of IPA.

When the PDMS membrane matrix was incorporated with the ZSM-5 zeolite, DS increased more than that of the virgin membrane. This effect became more prominent as the zeolite content increased in the membrane matrix and can be clearly seen for membranes M to M-3 in Figure 2. This was expected because ZSM-5 zeolite is basically hydrophobic in nature and increasing the zeolite in the membrane matrix obviously increased the

hydrophobic properties of the membranes. As a result, the ability of the membranes to absorb the IPA molecules increased, and this was responsible for greater swelling with increasing zeolite content in the membranes.

#### **Effects of the feed composition and zeolite loading on the PV properties**

As pointed out by Mulder and Smolders,<sup>26</sup> the permeation of liquid molecules through a rubbery polymer

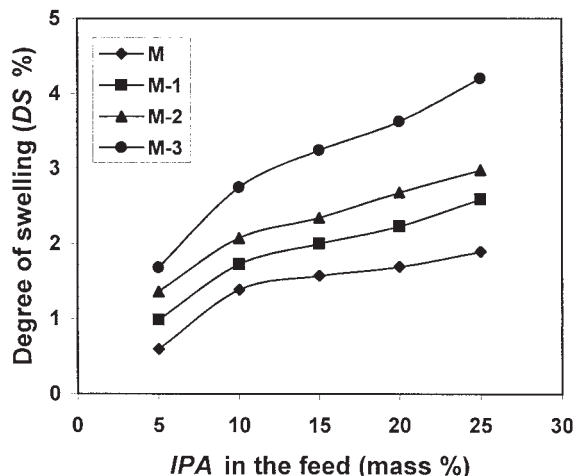


Figure 2 Variation of DS with different mass percentages of IPA in the feed for pure and zeolite-incorporated membranes.

occurs via a solution-diffusion mechanism. It is driven by a concentration gradient between the two surfaces of a membrane. During permeation, the liquid molecules absorb on one side of the membrane, diffuse across it, and desorb from the opposite side. On the basis of the qualitative description, we can say that the permeability is a function of both the solubility and diffusivity of liquid molecules in the membrane material. To enhance the membrane performance, we can try to improve the selective sorption, to lower the diffusion barrier, or to do both. In this study, we have concentrated on the former concept by improving the preferential sorption of the membranes.

Figure 3 shows the effect of the feed composition on the total permeation flux for all the membranes at 30°C. The permeation flux increased linearly for all the

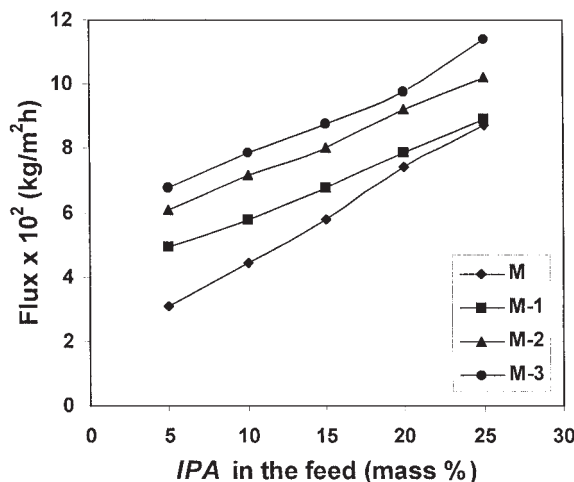


Figure 3 Variation of the total flux with different mass percentages of IPA for pure and zeolite-incorporated membranes.

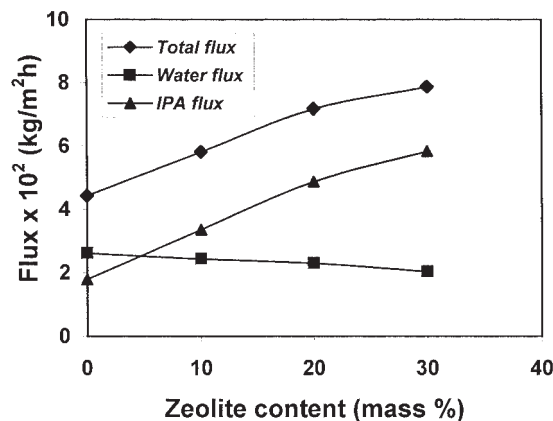
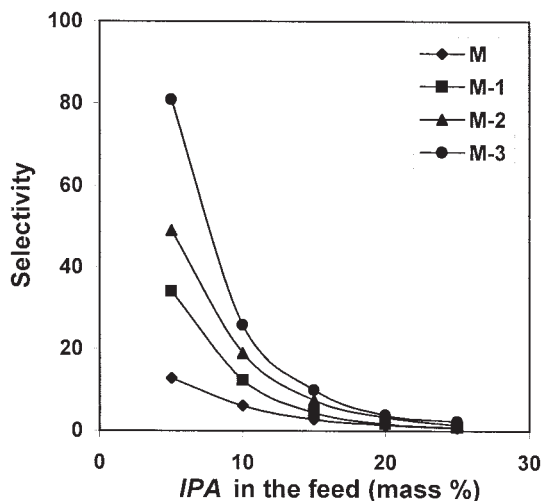


Figure 4 Variation of the total flux and the fluxes of water and IPA with different mass percentages of zeolite in membranes with 10 mass % IPA in the feed.

membranes, regardless of the zeolite loading, with increasing IPA concentration in the feed. This was due to increased interaction between the membranes and IPA molecules. On the other hand, the permeation flux increased systematically with respect to the zeolite loading (M to M-3) because the addition of an adsorptive filler to a polymer matrix is known to improve the selective property of a membrane in addition to the creation of a smooth path for the diffusion of selective molecules. As a result, the permeation flux increased greatly for all the membranes with all the investigated IPA compositions.

On the basis of the permeation of individual components, we can assess the efficiency of the membranes in the PV process. Thus, the extent of the permeation of individual components was determined by the plotting of the total flux and the fluxes of water and IPA as a function of the zeolite content in the membranes with 10 mass % IPA in the feed, as shown in Figure 4. With increasing zeolite content in the membranes, both the total flux and flux of IPA increased almost in parallel, and the water flux was suppressed; this suggested that the membranes developed in this study were selective toward IPA molecules. Furthermore, the pure membrane exhibited higher water flux than IPA flux, but this was suppressed significantly by the incorporation of the zeolite and its loading in the membrane matrix. This clearly reveals that the zeolite and its quantity incorporated into the membranes are solely responsible for enhancing the membrane performance through selective transport.

The overall selectivity of a membrane in the PV process is generally explained by the interaction between the membrane and permeating molecules, the molecular size of the permeating species, and the pore diameter of the membrane. Figure 5 displays the effects of the IPA compositions on the selectivity of all



**Figure 5** Variation of the separation selectivity with different mass percentages of IPA in the feed for pure and zeolite-incorporated membranes.

the membranes. Although the selectivity decreased for all the membranes with increasing IPA concentration in the feed, it was more predominant for the membranes with higher zeolite loadings. This was because of greater swelling due to increased selective interactions between the zeolite-loaded membrane and IPA molecules.

On the contrary, the selectivity increased significantly from membrane M-1 to M-3 with increasing zeolite content in the membrane throughout the investigated range of IPA compositions. This was attributed to increased selective interactions between the membrane and IPA molecules with increasing zeolite content in the membrane matrix. This can be clearly seen

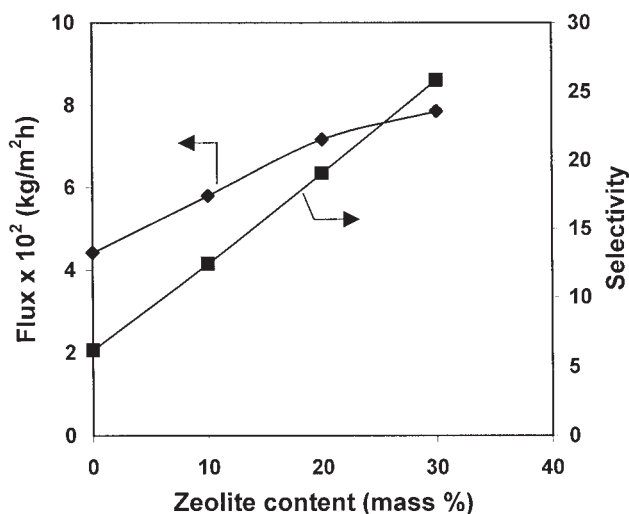


**Figure 6** Variation of the total flux and selectivity with different mass percentages of zeolite in membranes with 10 mass % IPA in the feed.

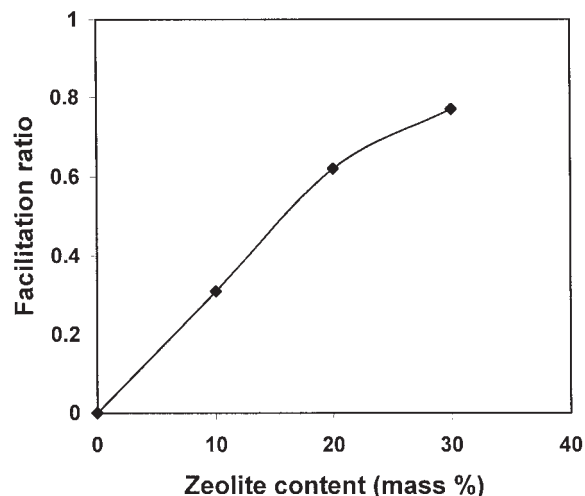


**Figure 7** Variation of the facilitation ratio with different mass percentages of zeolite in membranes with 10 mass % IPA in the feed.

in Figure 6, in which the flux and selectivity are plotted as functions of the zeolite content in the membranes with 10 mass % IPA in the feed. Both the permeation flux and selectivity increased with increasing zeolite content in the membranes. Generally, as the packing density of membranes increases either because of an increase in the crosslinking density or because of the incorporation of the zeolite into the membrane matrix, the permeation flux decreases and the selectivity increases.<sup>4,13</sup> However, in this study, both the permeation flux and selectivity increased simultaneously with increasing zeolite content in the membranes. Although this was in contrast to a tradeoff phenomenon existing between the flux and separation factor in the PV process, a significant enhancement of the hydrophobicity, selective adsorption, and the establishment of a molecular sieving action in the membrane matrix overcame the situation.

To understand the molecular sieving effect on the permeabilities for zeolite-incorporated membranes, we have calculated the facilitation ratio with the following equation proposed by Jia et al.<sup>14</sup> with 10 mass % IPA in the feed:

$$(P_{z+p} - P_p) / P_p \quad (5)$$

where  $P_{z+p}$  and  $P_p$  are the permeability of zeolite-filled and zeolite-free membranes, respectively. The resulting facilitation ratios are presented in Figure 7. The facilitation ratio increased linearly with increasing zeolite loading in the membrane matrix, and this indicated that the molecular sieving effect significantly contributed to the permeability. This agreed with the results observed in Figures 3 and 6.

The results for the total flux and selectivity and the fluxes of water and IPA measured at 30°C for all the

**TABLE II**  
Pervaporation Flux and Separation Selectivity Data for Different Mass Percentages of Isopropanol in the Feed at 30°C for Different Membranes

Mass % of IPA	$J \times 10^2$ (kg m <sup>-2</sup> h <sup>-1</sup> )				$\alpha_{sep}$			
	M	M-1	M-2	M-3	M	M-1	M-2	M-3
5	3.07	4.95	6.09	6.78	12.88	34.09	49.08	80.84
10	4.42	5.80	7.17	7.86	6.18	12.40	19.05	25.84
15	5.77	6.78	8.01	8.76	2.83	4.55	7.45	9.99
20	7.44	7.86	9.23	9.78	1.53	1.78	3.40	3.90
25	8.73	8.93	10.23	11.40	0.76	0.89	1.47	2.32

membranes with the investigated feed compositions are presented in Tables II and III, respectively. There was a systematic increase in the total flux with respect to both the IPA composition and zeolite loading. Similarly, the selectivity increased systematically with an increasing amount of the zeolite throughout the investigated range of water concentrations, but it decreased with respect to the IPA concentration. With respect to the individual fluxes, the flux of IPA increased from membrane M to M-3, but the flux of water was suppressed. This was due to an increase in the hydrophobic properties of the membranes with the incorporation of the zeolite. On the contrary, the water flux of the zeolite-incorporated membranes increased with increasing IPA concentration in the feed, but the IPA flux was suppressed. As the concentration of IPA increased in the feed, the interaction between the IPA molecules and membranes was greatly enhanced, and so the IPA molecules were bound with the membrane matrix. This resulted in the suppression of the diffusion of the IPA molecules. On the contrary, this situation favored the diffusion of water molecules significantly and resulted in a higher water flux for all the membranes with increasing IPA concentration.

#### Effect of the zeolite loading on PSI

PSI is the product of the total permeation and separation factor, which characterizes the membrane separation ability. This index can be used as a relative guideline for the design of a membrane in PV separation processes and also for the selection of a membrane

with an optimal combination of flux and selectivity. Figure 8 shows the variation of PSI as a function of the zeolite content in the membranes with 10 mass % IPA in the feed at 30°C. The PSI values increased exponentially with increasing zeolite content, and this signified that the membranes incorporated with a higher amount of zeolite showed better performance while separating the IPA/water mixtures. This was attributed to the incorporation of the zeolite into the membrane matrix, which changed not only the hydrophobicity of the membranes but also their morphology, which may have a significant influence on diffusion. Sorption was only the first step; in the second step of diffusion, the unique property of the zeolite and its significant role in the membrane matrix improved the overall permeation performance of the membranes.

On the basis of the significant performance and stability of the membranes shown in this system, we plan to use these membranes for the separation of lower alcohols such as methanol and ethanol, including other organic molecules such as acetic acid, tetrahydrofuran, and dioxan, in a future study.

#### Diffusion coefficient

The transport of binary liquid molecules in PV experiments is generally explained by the solution-diffusion mechanism, which occurs in three steps: sorption, diffusion, and evaporation.<sup>27</sup> Thus, the permeation rates and selectivity are governed by the solubility and diffusivity of each component of the feed mixture to be separated. In the process, because of the establish-

**TABLE III**  
Pervaporation Fluxes of Water and Isopropanol ( $J_w$  and  $J_{IPA}$ , Respectively) at Different Mass Percentages of IPA in the Feed at 30°C for Different Membranes

Mass % of IPA	$J_w \times 10^2$ (kg m <sup>-2</sup> h <sup>-1</sup> )				$J_{IPA} \times 10^2$ (kg/m <sup>2</sup> h)			
	M	M-1	M-2	M-3	M	M-1	M-2	M-3
5	1.83	1.77	1.70	1.29	1.24	3.18	4.39	5.49
10	2.62	2.44	2.30	2.03	1.80	3.36	4.87	5.83
15	3.85	3.76	3.46	3.17	1.92	3.02	4.55	5.59
20	5.38	5.44	4.99	4.95	2.06	2.42	4.24	4.83
25	6.97	6.89	6.87	6.44	1.76	2.04	3.36	4.96

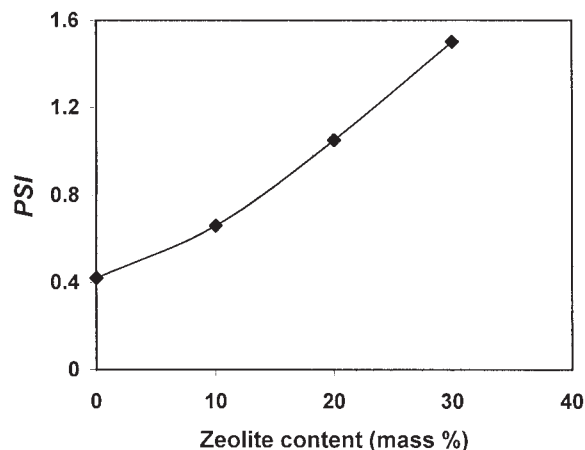


**Figure 8** Variation of PSI with different mass percentages of zeolite in membranes with 10 mass % IPA in the feed.

ment of the fast equilibrium distribution between the bulk feed and the upstream surface of a membrane,<sup>4,28</sup> the diffusion step controls the transport of penetrants. Therefore, it is important to estimate the diffusion coefficient of penetrating molecules to understand the mechanism of molecular transport.

From Fick's law of diffusion, the diffusion flux can be expressed as follows:<sup>29</sup>

$$J_i = -D_i \frac{dC_i}{dx} \quad (6)$$

where  $J_i$  is the permeation flux per unit of area of water or IPA ( $\text{kg}/\text{m}^2 \text{ s}$ ),  $D_i$  is the diffusion coefficient of water or IPA ( $\text{m}^2/\text{s}$ ),  $C$  is the concentration of the permeate ( $\text{kg}/\text{m}^3$ ), subscript  $i$  stands for water or IPA, and  $x$  is the diffusion length (m). For simplicity, it is assumed that the concentration profile along the diffusion length is linear. Thus,  $D_i$  can be calculated with the following equation:<sup>7</sup>

$$D_i = \frac{J_i \delta}{C_i} \quad (7)$$

where  $\delta$  is the membrane thickness. The calculated diffusion coefficients at 30°C are presented in Table IV. Similarly to the PV study, the diffusion coefficients of IPA increased significantly from membrane M to M-3, and the diffusion coefficients of water were suppressed. This showed that the membranes developed in this study had remarkable separation ability for the separation of water/IPA mixtures, particularly at lower concentrations of IPA in the feed. This was attributed to increased selective adsorption and the establishment of molecular sieving action by the incorporation of zeolite into the membrane matrix. However, the diffusion coefficients of IPA decreased for all the membranes with increasing IPA concentration in the feed. Such a decrease is known to occur because of greater interaction between the membrane and IPA molecules. This effect became more predominant as the IPA concentration increased in the feed because the IPA molecules were held with the membrane matrix and, as a result, the diffusion of IPA decreased greatly. On the contrary, to compensate for this, the diffusion of water molecules increased with increasing IPA concentration in the feed. Nevertheless, the magnitude of the diffusion coefficient of IPA was quite high in comparison with that of water, and this suggested that the membranes developed in this study were still selective toward IPA molecules even at higher concentrations of IPA in the feed.

#### Effect of the temperature on the membrane performance

The temperature is another important factor affecting the PV process in all the steps: sorption, diffusion, and desorption. Generally, the flux increases as the temperature increases, and the overall temperature effect on the partial flux at a fixed condition can usually be described with an Arrhenius expression. The separation efficiency of the membrane will thus be dependent on the overall activation energy of each permeant.

The effect of the operating temperature on the PV performance was studied for water/IPA mixtures with 10 mass % IPA in the feed, and the resulting

**TABLE IV**  
Diffusion Coefficients of Water and Isopropanol ( $D_w$  and  $D_{\text{IPA}}$ , Respectively) Calculated from Eq. (7) at Different Mass Percentages of IPA in the Feed for Different Membranes

Mass % of IPA	$D_w \times 10^8$ ( $\text{m}^2/\text{s}$ )				$D_{\text{IPA}} \times 10^7$ ( $\text{m}^2/\text{s}$ )			
	M	M-1	M-2	M-3	M	M-1	M-2	M-3
5	0.77	0.75	0.72	0.54	3.34	8.68	12.09	14.62
10	1.17	1.08	1.02	0.90	2.42	4.54	6.61	6.79
15	1.82	1.77	1.63	1.49	1.72	2.69	4.09	4.25
20	2.69	2.73	2.49	2.48	1.38	1.62	2.85	2.99
25	3.72	3.69	3.67	3.45	0.94	1.09	1.80	2.24



TABLE V  
Pervaporation Flux and Separation Selectivity at Different Temperatures for Different Membranes with 10 Mass % IPA in the Feed

Temperature (°C)	$J \times 10^2$ (kg/m <sup>2</sup> h)				$\alpha_{\text{sep}}$			
	M	M-1	M-2	M-3	M	M-1	M-2	M-3
30	4.42	5.80	7.17	7.86	6.18	12.40	19.05	25.84
40	6.57	9.49	12.90	13.39	4.65	9.75	11.93	16.00
50	9.49	12.1	13.20	13.76	4.00	8.65	10.15	11.22

values are presented in Table V. The permeation rate increased from 30 to 50°C, whereas the separation factor decreased. This was because of increasing thermal energy, which increased the free volume in the membrane matrix on account of the increased frequency and amplitude of the polymer chain jumping.<sup>30</sup> As a result, the diffusion of both permeating molecules increased, and this led to higher flux, whereas the selectivity was suppressed. This effect prompted us to estimate the activation energies for permeation ( $E_p$ ) and diffusion ( $E_D$ ) with an Arrhenius-type equation:<sup>31</sup>

$$X = X_0 \exp\left(\frac{-E_x}{RT}\right) \quad (8)$$

where  $X$  represents permeation ( $J$ ) or diffusion ( $D$ );  $X_0$  is a constant representing the pre-exponential factor ( $J_0$  or  $D_0$ );  $E_x$  represents  $E_p$  or  $E_D$ , depending on the transport process under consideration; and  $RT$  is the usual energy term. As the feed temperature increased, the vapor pressure in the feed compartment (upstream side) also increased, but the vapor pressure at the permeate side (downstream side) was not affected. All this resulted in an increase in the driving force with increasing temperature.

$E_p$  and  $E_D$  mainly depend on the membrane morphology. Generally, zeolite-incorporated membranes have lower  $E_p$  and  $E_D$  values than a pure membrane because of the formation of pores in the membrane matrix. Arrhenius plots of  $\log J$  versus  $1/T$  and  $\log D$  versus  $1/T$  are shown in Figures 9 and 10 for the temperature dependence of the permeation flux and diffusion, respectively. In both cases, linear behavior was observed, and this suggested that both permeability and diffusivity followed an Arrhenius trend. From least-squares fits of these linear plots,  $E_p$  and  $E_D$  were estimated, and the results thus obtained are presented in Table VI. The pure membrane (M) exhibited higher  $E_p$  and  $E_D$  values than the zeolite-incorporated membranes (M-1 to M-3). This suggested that both permeating and diffusing molecules required more energy for transport through M because of its dense nature. Obviously, zeolite-incorporated membranes take less energy because of a molecular sieving action attributed to the presence of straight and sinusoidal channels in the framework of the zeolite.<sup>4</sup> Therefore,  $E_p$  and  $E_D$  decreased systematically from membrane M-1 to M-3 with increasing zeolite content.

The  $E_p$  and  $E_D$  values ranged between 21.81 and 31.12 kJ/mol and between 15.27 and 41.49 kJ/mol,

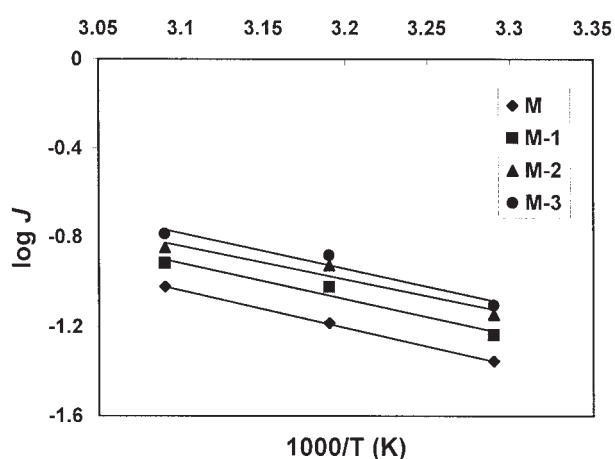


Figure 9 Variation of  $\log J$  with the temperature for pure and zeolite-incorporated membranes with 10 mass % IPA in the feed.

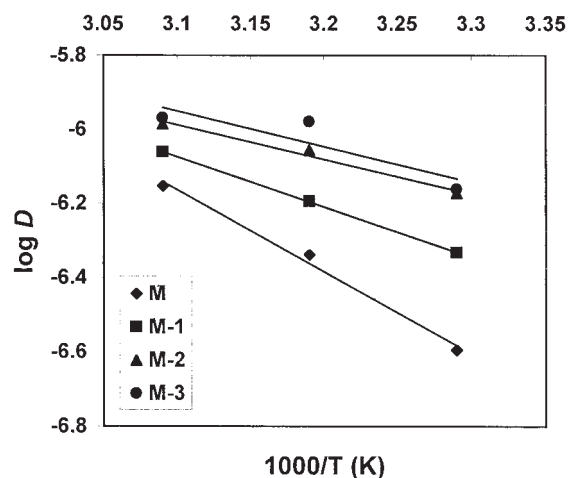


Figure 10 Variation of  $\log D$  with the temperature for pure and zeolite-incorporated membranes with 10 mass % IPA in the feed.

TABLE VI  
Arrhenius Activation Parameters for Permeation  
and Diffusion and  $\Delta H_s$

Parameter (kJ/mol)	M	M-1	M-2	M-3
$E_p$	31.12	30.05	23.63	21.81
$E_D$	41.49	25.45	17.56	15.27
$\Delta H_s$	-10.37	4.6	6.07	6.54
$E_{pw}$	21.62	36.39	45.79	54.63
$E_{pIPA}$	41.94	24.74	9.85	8.21

respectively. Using these values, we calculated the heat of sorption ( $\Delta H_s$ ) as follows:

$$\Delta H_s = E_p - E_D \quad (9)$$

The resulting  $\Delta H_s$  values are included in Table VI. Generally,  $\Delta H_s$  is a composite parameter involving contributions of both Henry's type of sorption and Langmuir's type of sorption.<sup>32</sup> Henry's mode requires both the formation of a site and the dissolution of chemical species into that site. The formation of a site involves an endothermic contribution to the sorption process. In case of Langmuir's mode, the site already exists in the polymer matrix, and consequently, sorption occurs by a hole-filling mechanism, making an exothermic contribution. However, the  $\Delta H_s$  values obtained in this study were positive for all the zeolite-incorporated membranes, despite the existing pores. Although this is contrary to the general observation, it may have occurred because of a greater interaction between the IPA molecules and membranes. This consumed more energy for permeation through the zeolite-incorporated membranes, and this suggests that Henry's sorption was predominant, making an endothermic contribution. On the contrary, the  $\Delta H_s$  value observed for the pure membrane was negative, and this suggests that Langmuir's sorption dominated because of less interaction between the permeating molecules and the membrane in comparison with the zeolite-incorporated membranes.

Furthermore, we estimated the apparent activation energies for water permeation ( $E_{pw}$ ) and IPA permeation ( $E_{pIPA}$ ), and these values are also included in Table VI. For the zeolite-incorporated membranes, the  $E_{pIPA}$  values were much lower than the  $E_{pw}$  values, and this suggests that the zeolite-incorporated membranes had higher selectivity toward IPA. This was in good agreement with the results observed in Figure 4.

## CONCLUSIONS

PDMS membranes, incorporated with greater amounts of ZSM-5 zeolite, showed better performance during the separation of water/IPA mixtures. An increase in the zeolite content in the membranes resulted

in a simultaneous increase in both the permeation flux and selectivity. This was attributed to a significant enhancement of the hydrophobic character, selective adsorption, and the establishment of a molecular sieving action. The PSI data also indicated that the higher the zeolite loading was, the better the membrane performance was. This was due to significant changes in the hydrophobicity of the membranes, including the morphology. The highest separation selectivity was 80.84 with a flux of  $6.78 \times 10^{-2} \text{ kg m}^{-2} \text{ h}^{-1}$  for the membrane with the highest loading of zeolite at 30°C with 5 mass % IPA in the feed. With respect to the temperature effect, the permeation rate increased, and the selectivity was suppressed, when the temperature was increased. This phenomenon was attributed to an increase in the frequency and amplitude of polymer chain jumping in the membrane matrix due to thermal energy. In comparison with the zeolite-incorporated membranes, the pure membrane had higher  $E_p$  and  $E_D$  values, and this signified that permeation and diffusion required more energy for the transport of permeating molecules through the pure membrane because of its dense nature. Naturally, the zeolite-incorporated membranes required less energy because of their molecular sieving action, which was attributed to the presence of straight and sinusoidal channels in the framework of the zeolite. The estimated  $E_{pIPA}$  values were significantly lower than the  $E_{pw}$  values. This revealed that the zeolite-incorporated membranes were highly selective toward IPA. The estimated  $E_p$  and  $E_D$  values ranged between 21.81 and 31.12 kJ/mol and between 15.27 and 41.49 kJ/mol, respectively. All the zeolite-incorporated membranes exhibited positive  $\Delta H_s$  values, and this suggested that sorption was dominated by Henry's mode of sorption, making an endothermic contribution.

The authors thank Wacker-Chemie GmbH (Germany) for kindly supplying the poly(dimethyl siloxane) samples.

## References

1. Lin, X.; Kita, H.; Okamoto, K. *Ind Eng Chem Res* 2001, 40, 4069.
2. Karlsson, H. O. E.; Tragardh, G. *J Membr Sci* 1993, 76, 121.
3. Neel, J. In *Pervaporation Membrane Separation Processes*; Huang, R. Y. M., Ed.; Elsevier: Amsterdam, 1994.
4. Kittur, A. A.; Kariduraganavar, M. Y.; Toti, U. S.; Ramesh, K.; Aminabhavi, T. M. *J Appl Polym Sci* 2003, 90, 2441.
5. Sarkhel, D.; Roy, D.; Bandyopadhyay, M.; Bhattacharya, P. *Sep Purif Technol* 2003, 30, 89.
6. George, S. C.; Ninan, K. N.; Thomas, S. *J Membr Sci* 2000, 176, 131.
7. Kusumocahyo, S. P.; Sudoh, M. *J Membr Sci* 1999, 161, 77.
8. Kariduraganavar, M. Y.; Kulkarni, S. S.; Kittur, A. A. *J Membr Sci* 2005, 246, 83.
9. Lin, X.; Kikuchi, E.; Matsukata, M. *Chem Commun* 2000, 957.
10. Nam, S. Y.; Chun, H. J.; Lee, Y. M. *J Appl Polym Sci* 1999, 72, 241.
11. Moon, G. Y.; Pal, R.; Haung, R. Y. M. *J Membr Sci* 1999, 156, 17.

12. Kulkarni, S. S.; Kittur, A. A.; Aralaguppi, M. I.; Kariduraganavar, M. Y. *J Appl Polym Sci* 2004, 94, 1304.
13. Kurkuri, M. D.; Toti, U. S.; Aminabhavi, T. M. *J Appl Polym Sci* 2002, 86, 3642.
14. Jia, M.; Peinemann, K. V.; Behling, R. D. *J Membr Sci* 1991, 57, 289.
15. te Hennepe, H. J. C.; Bargeman, D.; Mulder, M. H. V.; Smolders, C. A. *J Membr Sci* 1987, 35, 39.
16. Kim, K. J.; Park, S. H.; So, W. W.; Moon, S. J. *J Appl Polym Sci* 2001, 79, 1450.
17. Paul, D. R.; Kemp, D. R. *J Polym Sci Polym Symp* 1973, 41, 79.
18. Kulprathipanja, S.; Neuzil, R. W.; Li, N. N. U.S. Pat. 4,740,219 (1988).
19. te Hennepe, H. J. C.; Mulder, M. H. V.; Smolders, C. A.; Bargeman, D.; Schroder, G. A. T. Eur. Pat. 0,254,758 (1988).
20. Suzuki, H. Eur. Pat. 0,180,200 (1985).
21. Rojey, A.; Deschamps, A.; Grehier, A.; Robert, E. Eur. Pat. 0,324,675 (1989).
22. Vankelecom, I. F. J.; Beukelaer, S. D.; Uytterhoeven, J. B. *J Phys Chem B* 1997, 101, 5186.
23. Flanigen, E. M.; Bennett, J. M.; Grose, R. W.; Cohen, J. P.; Patton, R. L.; Kirchner, R. M.; Smith, J. V. *Nature* 1978, 271, 512.
24. Kariduraganavar, M. Y.; Kittur, A. A.; Kulkarni, S. S. *J Membr Sci* 2004, 238, 165.
25. Kittur, A. A.; Tambe, S. M.; Kulkarni, S. S.; Kariduraganavar, M. Y. *J Appl Polym Sci* 2004, 94, 2101.
26. Mulder, M. H. V.; Smolders, C. A. *J Membr Sci* 1984, 17, 289.
27. Lee, Y. M.; Bourgeois, D.; Belfort, G. *J Membr Sci* 1989, 44, 161.
28. Hwang, S. T.; Kammermeyer, K. *Membrane in Separations*; Wiley-Interscience: New York, 1975.
29. Yamasaki, A.; Iwatsubo, T.; Masuoka, T.; Misoguchi, K. *J Membr Sci* 1994, 89, 111.
30. Binning, R. C.; Lee, R. J.; Jennings, J. F.; Martin, E. C. *Ind Eng Chem* 1961, 53, 45.
31. Huang, R. Y. M.; Yeom, C. K. *J Membr Sci* 1991, 58, 33.
32. Weinkauf, D. H.; Paul, D. R. In *Barrier Polymers and Structures*; Koros, W. J., Ed.; ACS Symposium Series 423; American Chemical Society: Washington, DC, 1990.